

SIMULTANEOUS REMOVAL OF METHYLENE BLUE DYE AND WATERBORNE PATHOGENS FROM WASTEWATER USING EXTRACT OF *EMBELIA SCHIMPERI* FRUITS

Belete Tewabe Gebeyehu, Minbale Gashu Tadesse and Abebe Tedla*

Department of Chemistry, Debre Berhan University, Debre Berhan, Ethiopia

(Received September 9, 2023; Revised November 22, 2023; Accepted December 12, 2023)

ABSTRACT. In this study, we report the use of *Embelia schimperi* fruits'extract to simultaneously remove methylene blue dye and pathogens from wastewater. The extract of *Embelia schimperi* fruits was characterized by Atomic force Microscopy and Fourier Transform Infra-Red spectroscopy. The adsorption properties of the crude extracts of the fruits were explored as a function of dosage, contact time, pH, initial methylene blue concentrations, and temperature. As a result, the highest removal efficiency of methylene blue was found to be 99.2% at optimum conditions. The adsorption data demonstrated that the adsorption of *Embelia schimperi* followed the Langmuir isotherm model ($R^2 = 0.94899$) and the pseudo-second-order kinetic model ($R^2 = 0.99326$). Besides, crude extracts of the fruits showed significant antibacterial properties against gram-positive and gram-negative bacteria. Agar diffusion tests confirmed that *Listeria monocytogenes* and *Staphylococcus aureus* were highly sensitive to the crude extracts of *Embelia schimperi* fruits, followed by *Escherichia coli* and *Salmonella typhi*. Thus, the findings of this study confirm the promising potential of *Embelia schimperi* fruits as a natural adsorbent used to remove methylene blue dye and pathogenic bacteria at the same time from wastewater.

KEY WORDS: *Embelia schimperi*, Adsorption, Isotherm, Kinetic, Methylene blue, Waterborne pathogens

INTRODUCTION

The amount of pollutants found in water has increased along with industry, urbanization, and human activity [1, 2]. The environment has been severely harmed by the excessive release of dyes, heavy metals, and household waste [2]. It is undeniable that the widespread use of synthetic dyes in industries such as textiles, leather, cosmetics, paper, paper production, pharmaceuticals, printing, food, etc. is having a significant negative impact on human and other animal life around the world [2].

Methylene blue (MB), for instance, is used to dye cotton, wool, paper, and other materials as well as to color hair [3]. Although it has a broader range of uses, methylene blue dye harms living systems in a number of ways. Diarrhea, vomiting, nausea, chest discomfort, increased heart rate, breathing difficulties, burning in the mouth, rapid headaches, eye burns, and gastritis are all side effects of this dye [3, 4].

As a result, environmentalists are continuously faced with the challenge of handling wastewater that contains notorious cationic dyes in a safe and efficient manner. Until date, a variety of conventional methods such as chemical oxidation or reduction [5, 6], filtration, evaporation, coagulation–flocculation [7], adsorption [5], electrochemical treatment [8] and ion exchange [9] have been employed to remove the contaminants from wastewater. But because of their high cost, inefficiency, and difficulty in use, these procedures are frequently impractical. Adsorption among these is a suitable technique for removing dye pollutants from water due to its high efficiency, affordability, and simplicity of use.

A variety of adsorbents [10-13] made from natural materials have been thoroughly investigated by numerous researchers in batch experiments for pollutant adsorption; however, there is still room for improvement in terms of their efficiency and environmentally friendly

*Corresponding author. E-mail: abebetedla@gmail.com

This work is licensed under the Creative Commons Attribution 4.0 International License

approach. Therefore, it is critical to discover more affordable substitute materials for the quick and effective removal of dyes from wastewater treatment operations.

In addition to dyes, several bacteria and parasites that are prevalent microorganisms affecting human health also contribute to water contamination [14, 15]. Humans who consume water that has been contaminated by microbes often develop gastrointestinal diseases. The fact that some bacterial illnesses are resistant to several medications makes them particularly challenging to treat with conventional therapies [1, 15, 16]. For instance, *Salmonella typhi*, *Staphylococcus aureus*, and *Escherichia coli* are types of bacteria that are frequently found in contaminated water [15-17]. These bacteria are suspected of being the source of diseases such as typhoid fever, septicemia, boils, dysentery, and diarrhea [15]. Consequently, microbiological contamination has always been a risk to human health; as a result, it is necessary to treat such toxic wastewater with efficient and environmentally friendly techniques.

Despite the fact that the majority of adsorbents have shown adequate adsorptive potential, only few materials such as chitosan [18] and *Moringa oleifera* seeds [19] have antibacterial properties. Thus, various researchers are interested in finding adsorbents that can be used in the removal of dyes as well as the disinfection of wastewater.

The plant *Embelia schimperi* Vatke, known by its local name “*Enkoko*” belongs to the family Myrsinaceae. This plant is a widespread climbing or creeping shrub in the highlands of tropical Africa. The fruits, seeds, or roots of the plant have long been traditionally used as an antibacterial and anthelmintic medication [16, 20] particularly for diarrhea and tapeworm [21]. For example, in Ethiopia, the seeds of *Embelia schimperi* (*E. schimperi*) are dried, powdered, and eaten to eliminate hookworms and tapeworms.

The reasons for wide range of applications in ethno-pharmacology is that the seeds of *Embelia* species contain a wide spectrum of bioactive constituents including embelin, christembin, several fatty acids, biembeline, vilangin, methyl vilangin [22], embelinol, embeliaribyl ester, embeliol, tannins, flavonoids, quercitol and sugars. There has been substantial study on pollutant adsorption using a variety of adsorbents derived from synthetic and natural materials; however, to the best of our knowledge, there is no report on the utilization of *E. schimperi* fruit extract to remove dyes like methylene blue (MB) from wastewater. Most importantly, there is no scholarly work that has demonstrated the dual effects (adsorbing methylene blue dye and killing bacteria) of *E. schimperi* fruits. Therefore, the objective of this work is to investigate the potential of the chloroform extract of *E. schimperi* fruits in removing both pathogenic bacteria and methylene blue simultaneously from waste water.

EXPERIMENTAL

Chemicals

Dimethyl sulfoxide (DMSO), chloroform, and methylene blue were purchased from SD Fine-Chem Ltd., India. Gentamicin was obtained from Hindustan Antibiotics, India. All of the chemicals utilized in this study were of the highest purity and quality for analysis.

Preparation of adsorbent

The fruits of *E. schimperi* (Figure 1) used in this study were collected from the localities in Gojjam, Northwest Ethiopia. The collected *E. schimperi* samples were allowed to air dry at room temperature (Figure 1). Using an electric grinding mill, the dried berries of *E. schimperi* were ground into powder, and the powder was then sieved through a 4 mm mesh (No. 5). In the maceration process, 100 g of *E. schimperi* powdered fruits were extracted in 250 mL of chloroform using a conical flask. The conical flask's contents were kept at room temperature for 72 hours while being frequently shaken. The organic solvent was then recovered from the filtrate using a rotary evaporator (BUCHI B-205, Switzerland). After that, the extract was dried out in an

oven at room temperature. The dried extract obtained was measured, labeled, packed in a plastic bag, and stored at room temperature until needed.

Test organism

Using the American Type Culture Collection (ATCC), antimicrobial activity was assessed against four common bacterial strains collected from an Ethiopian public health institution (Addis Ababa). Gram-positive and Gram-negative bacterial strains that are frequently found in polluted water were chosen as representatives of both classes of these microorganisms. The disk diffusion antimicrobial test was conducted using the chosen microbial strains, including *Staphylococcus aureus* (SA, ATCC 29213), *Listeria monocytogenes* (LM, ATCC 19115), *Escherichia coli* (EC, ATCC 25922), and *Salmonella enteritidis* (SE, ATCC 13311).

Disc diffusion assay

The disc diffusion method was used to test the antibacterial activity of chloroform extracts of the fruits of *E. schimperi* on the chosen bacteria's standard strains. 100 μ L of bacterial culture was spread on the nutrient agar plates. On the cultivated plates, sterile filter paper discs (6 mm in diameter) were inserted and then incubated at 37 °C with 10 μ L of the *E. schimperi* fruit extract (25–100 mg/mL). The common antibiotic gentamycin (10 μ g/disc) was used as a positive control, and DMSO without extracts was employed as a negative control on the incubated plate. Then, it was incubated for 24 hours at 37 °C, and the average values of the zone of inhibition for antibacterial activity were measured in millimeters.

Instruments and characterization

The crude extracts of *E. schimperi* fruits were analyzed both before and after the methylene blue dye adsorption. The crude extract of the sample (0.01 g) was blended with KBr pellets and analyzed with the Fourier transform infrared (FTIR) spectroscopy (Alpha-T, Bruker spectrophotometer) within the range of 400–4000 cm^{-1} . To create the pellet, each sample was coarsely powdered, combined with KBr, and pressed.

The surface morphology of the crude extract of *E. schimperi* fruit (0.01 g) was examined using atomic force microscopy (AFM) on a tapping-mode (NX10, AFM Park Systems, Suwon, South Korea) fitted with a typical commercial silicon probe to assess the surface morphology before and after MB dye adsorption. Samples (0.4 g/L or 0.01 g) were prepared by spin coating 20 μ L of the dilute samples on the silicon substrate, followed by vacuum drying at 25 °C. The concentrations of MB dye solution were measured using a UV-Vis spectrophotometer (Jasco-V630) with an 800–200 nm measuring range and a 0.5 nm data interval.

Adsorption experiments

The dosage of the adsorbent, pH, initial MB concentrations, contact time, and temperature are variables that have an impact on the adsorption of the methylene blue dye onto extracts of the fruits of *E. schimperi*. For each adsorption system, MB adsorption experiments were done in batch mode under various experimental conditions, including dye initial concentration (10–100 mg/L), contact time (2–30 min), adsorbent dosage (0.005–0.1 g per 25 mL of MB solution), pH (2–10), and temperature (293–313 K) under 150 rpm shaking. The adsorption isotherm and kinetic studies were determined using MB adsorption's optimum conditions. For each experiment, after filtering the agitated adsorbate solution over a 0.22 μ m microfiltration membrane, the remaining MB dye concentrations in the filtrate were measured using a UV-VIS spectrophotometer at a pre-

optimized maximum wavelength of 664 nm. The initial pH was calibrated for each solution with a supplement of 0.1 M NaOH or 0.1 M HCl.

Equations (1), (2), and (3) were used to calculate the following data: percentage of removal (R %), amount of MB dye adsorbed at a given time (qt), and equilibrium (qe) by the adsorbent.

$$q_e = \frac{(C_o - C_e) \times V}{m} \quad (1)$$

$$q_t = \frac{(C_o - C_t) \times V}{m} \quad (2)$$

$$\% R = \frac{(C_o - C_t) \times 100}{C_o} \quad (3)$$

where C_o , C_t , and C_e are the concentrations of MB dye in mg/L at the beginning, after time t , and at equilibrium, respectively. R is the removal efficiency percentage, V is the MB volume in mL, and m is the *E. shimperi* biomass in g.

Determination of pH of point zero charge (pHpzc)

A conventional method was employed to estimate the pH of point zero charge (pHpzc) for *E. shimperi*. In a series of eleven flasks, each containing 25 mL of background electrolyte (0.01 mol L⁻¹ KNO₃), dried *E. shimperi* powder was added at a fixed mass of 0.01 g. The initial pH values were adjusted in the pH range of 2–11 using 0.1 mol L⁻¹ of HNO₃ or NaOH. The mixture obtained underwent vigorous shaking for 24 h at a speed of 150 rpm. Ultimately, the dispersions were filtered, and the final pH (pH_f) of the solution was determined. The pHpzc was found from a plot of pH_f vs pH_i. This procedure was repeated at various concentrations of 0.05 and 0.1 mol L⁻¹ KNO₃ solutions. The final pH was noted and plotted versus the initial pH, where the intersection point of the two curves determines the pHpzc of the biomass.

RESULTS AND DISCUSSION

Characterization of adsorbent

The ripped fruits (berries) were collected, dried, powdered, and subjected to maceration (Figure 1). The fruit of *E. shimperi* was subjected to maceration using a chloroform solvent. As shown in Figure 1, the crude extract *E. shimperi* (dark orange or brown color) was used to study the adsorbent characteristics and the effects of various factors that affect adsorption, as well as for the treatment of pathogens. Figure 1 shows the photograph of *E. shimperi* Vatke plant; dried fruits of *E. shimperi* fruits and crude extracts of *E. shimperi* fruits. Additionally, Figure 1 displays a diagrammatic illustration of how *E. shimperi* fruits' crude extract simultaneously removes methylene blue dye and pathogens from wastewater.

The surface morphologies of the crude extract of *E. shimperi* fruit were examined before and after MB adsorption using AFM (Figures 2a and 2b). The *E. shimperi* fruits exhibited a rough surface with visible pores of an average diameter of 123 nm before adsorption as shown in Figure 2a. The surface morphologies of *E. shimperi* fruits revealed that the majority of the pores was filled with the deposited MB dye after the adsorption of the MB dye (Figure 2b). Thus, on the basis of AFM images, it can be inferred that the *E. shimperi* fruit has suitable morphology for dye adsorption.

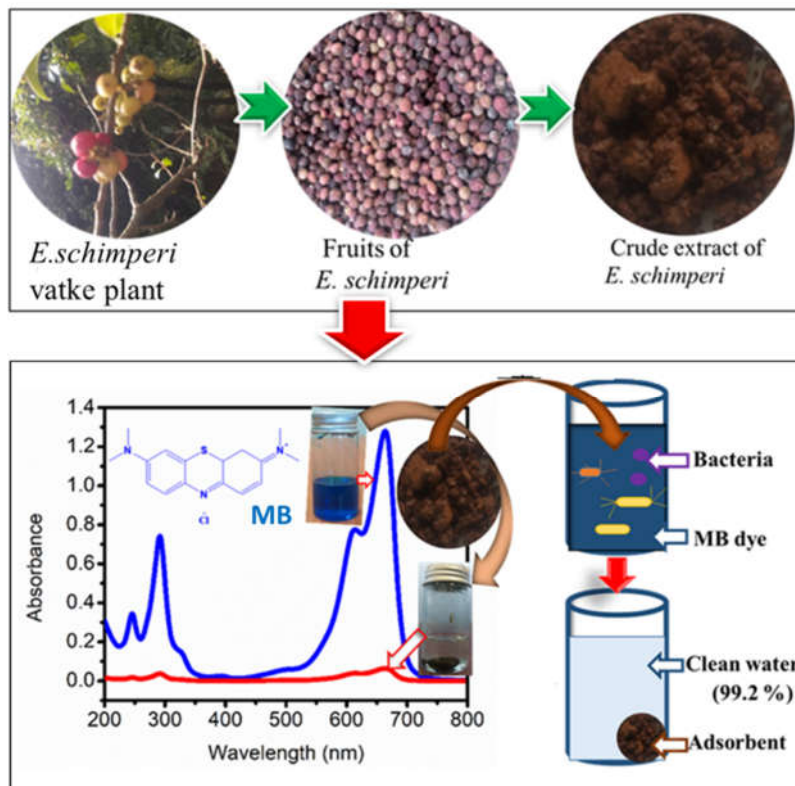


Figure 1. Images of *E. schimperi* plant with its crude extract, and diagrammatical illustration showing the removal of methylene blue and pathogens from wastewater using the extract.

FTIR spectroscopy was used to identify the various functional groups that were present on the surface of the fruits of *E. schimperi*. Figure 2c clearly illustrates that the extract of *E. schimperi* fruit is enriched with a number of functional groups that are available for the adsorption of dye. As demonstrated in Figure 2c, before the adsorption of MB dye, the crude chloroform extract of the biomass showed sharp and intense vibration at 3298 cm^{-1} attributed to the hydroxyl moiety (OH). The bands at 2921 cm^{-1} , 2853 cm^{-1} correspond to —CH_3 and —CH_2 due to C-H stretching of saturated moiety, respectively. The bands at 1714 and 1613 cm^{-1} assigned to the C=O stretching (assignable to stretching in esters and ketones, respectively) cm^{-1} to the asymmetric and symmetric stretching vibrations of ionic carboxylic groups (—COO—), respectively.

The participation of respective functional groups during adsorption is clearly seen from the change in intensity and peak positions of crude extract *E. schimperi* after adsorption of MB (Figure 2c). The FTIR spectrum displays the distinctive absorption peaks for the biomass sample prior to MB dye biosorption at 3298 , 2921 , 2853 , 1714 , 1613 , 1459 , 1326 , 1187 and 703 cm^{-1} were shifted to 3330 , 2921 , 2853 , 1718 , 1615 , 1459 , 1328 , 1186 and 702 cm^{-1} ; respectively after MB biosorption by the biomass. These shifts in peak indicate the involvement of respective functional groups in the adsorption of MB by *E. schimperi* during the biosorption process.

As shown in Figure 2c, the values of the bands may be shifted due to the interaction of the *E. shimperi* surface with the adsorbed MB dye, which results in a shift, absence, or change in the values of the characteristic bands in the FTIR spectrum. The spectral data reveals any differences in morphological features and surface properties caused by interactions between the functional group's adsorbent, *E. shimperi*, and MB dye.

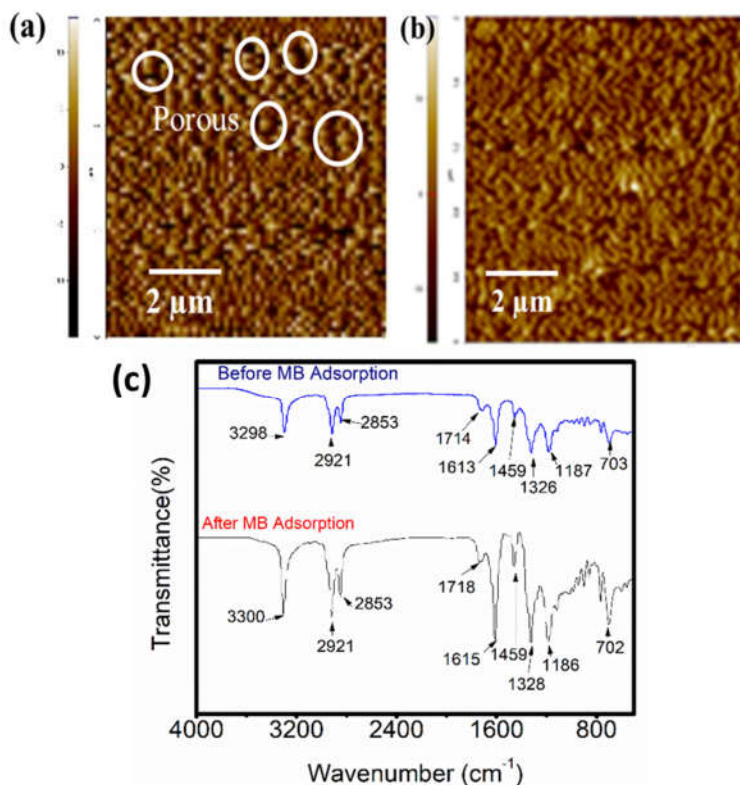


Figure 2. *E. shimperi* fruits (a) AFM image before adsorption; (b) AFM image after MB dye; and (c) FTIR spectra before and after adsorption.

Effect of various parameters on MB dye adsorption

The dose, the initial dye concentration, the pH, the contact time, and the temperature are some of the major factors that affect how dyes adhere to adsorbent surfaces. When the other variables are held constant, the impact of one parameter on the MB dye biosorption process can be observed. After describing the unloaded and loaded *E. shimperi*, a detailed analysis of how these factors affect the biosorption of MB cationic dye contaminants is briefly discussed as follows:

Effect of dose

In an effort to determine the lowest feasible dosage required for the highest possible adsorption of MB dye, the adsorbent dosage was varied, ranging from 0.2 to 4 g/L. Figure 3a displays the values of adsorption capacity and removal efficiency plotted against *E. shimperi* dosage at the

chosen experimental parameters of initial MB dye concentration (C_0) = 50 mg/L, temperature = 303 K, contact time = 20 min, pH = 8, and shaking rate of 150 rpm. When the adsorbent dose was increased from 0.2 to 0.4 g/L, the removal efficiency noticeably risen from 94% to 99.2 %, after which the increase was relatively small or negligible (99.8% at 4 g/L) (Figure 3a). On the other hand, with an increase in adsorbent dosage from 0.2 to 4 g/L, the adsorption capacity dramatically dropped from 235 to 13 mg/g (Figure 3a). The improvement in removal efficiency with increasing adsorbent doses may be caused by the availability of extra binding sites for adsorption. The adsorbent dose (0.4 g/L) had a removal efficiency of 99.2% with an adsorption capacity of 124.5 mg/g, which was selected for subsequent experiment.

Effect of contact time

Figure 3b illustrates how contact time alters MB dye removal and adsorption capacity under optimal conditions (dose = 0.4 g/L, initial MB dye concentration (C_0) = 50 mg/L, temperature = 303 K, pH = 8 and shaking rate 150 rpm). As shown in Figure 3b, the removal efficiency first increased from 40% to 96% as the time changed from 2 to 15 min, and it subsequently reached at 20 min (99.2%). Additionally, the adsorption capacity increased from 50 to 120 mg/L between 2 and 15 min, and equilibrium was almost achieved in 20 min (124.5 mg/g), after which there was little change in the adsorption capacity. The quick rise in adsorption capacity is observed in Figure 3b during the first 15 min may be caused by a higher availability of empty sites on the extracts of *E. schimperi* boundary layer. As the adsorption process progressed, fewer active sites were available, which caused the adsorption rate to rise more slowly. As a result, the establishment of a plateau after 20 min reveals a dynamic balance between the dye's adsorption and desorption [23]. The inset image in Figure 3b also shows how the MB dye discolors to varying degrees, from blue to colorless, based on how long the adsorbent and adsorbate are in contact with one another. The optimum time for the adsorption to reach equilibrium, as shown by the experimental data, is 20 min, and this time was chosen for optimum time.

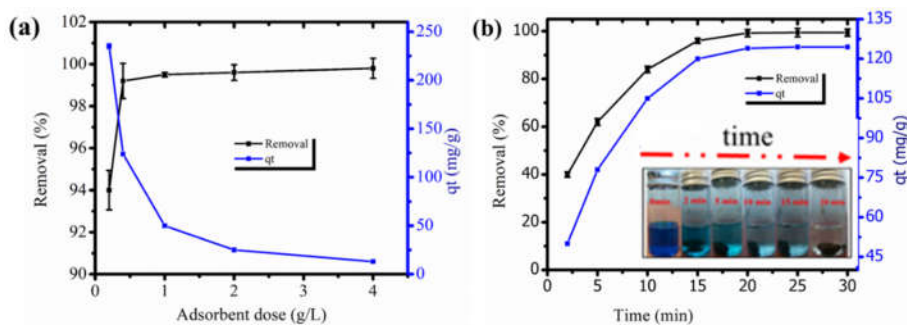


Figure 3. (a) The effect of the dose of adsorbent on the removal percentage and adsorption capacity; and (b) the effect of time on the removal percentage and adsorption capacity. The inset photograph shows the corresponding color change of the MB solutions at different time.

Effect of pH

For the experimental conditions of adsorbent dose = 0.4 g/L, C_0 = 50 mg/L, contact time = 20 min, and temperature = 303 K, the influence of pH on the adsorption efficiency is plotted in Figure 4a. The graph shows that the value of q_e was observed to increase from 51.2 mg/g to 124 mg/g as the pH of the medium was increased from 2 to 8. And also, removal efficiency increased from

41.3% to 99.2% with increasing pH, reaching its peak at pH = 8 (99.2%). Afterwards, removal efficiency did not change significantly as indicated in Figure 4a.

Therefore, in light of the aforementioned result, a pH value of 8 was determined to be the optimum one for subsequent study. It is pertinent to note in this context that an increase in pH resulted in an increase in the negative charge on the adsorbent surface, which deprotonates the functional group on the adsorbent, *E. schimperi*. As a result, these deprotonated functional groups act as the cationic MB's binding sites and accelerate adsorption. On the other hand, it appears that the lower dye adsorption in acidic media is caused by electrostatic repulsion between the positively charged adsorbent surface and the cationic MB dye. Similar results have been reported for different plant extracts, for instance, Indian rosewood sawdust [24], *Citrus limetta* peel [25] and yellow passion fruit peel [26] for the effects of the solution pH on the adsorption of MB.

An adsorbent property known as the point of zero charge can better explain the significant impact of pH on adsorption (pHpzc). The pHpzc of the *E. schimperi* adsorbent was 6.2, as shown in Figure 4b. This implies that at pH < 6.2, protonation charges the surface positively. While the deprotonation caused by many hydroxide ions at pH levels greater than 6.2 causes the adsorbent surface to become negatively charged. Thus, a value of 6.2 for pHpzc further indicates that the *E. schimperi* adsorbent favorably adsorbed any cationic dye at a pH of the medium greater than this value. Ionic interactions governed by the surface charges of the adsorbent and adsorbate in an aqueous solution cause the adsorption of cationic dye onto the adsorbent to occur.

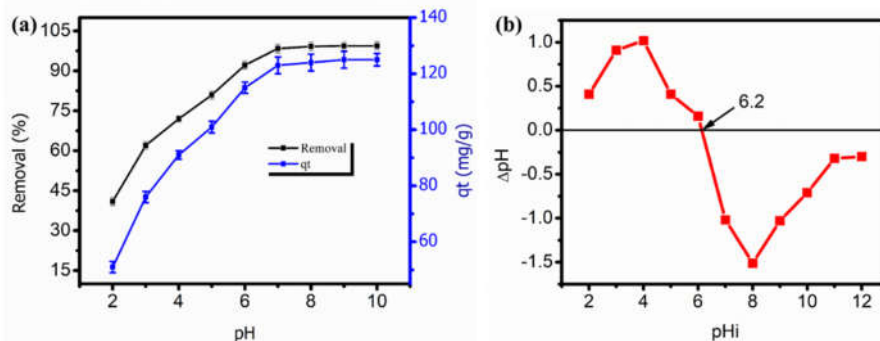


Figure 4. (a) The effect of pH on the removal percentage and adsorption capacity, and (b) The point of zero charge (pzc) for crude extracts of *E. schimperi* fruits.

Effect of initial concentration of MB dye

In order to assess the effect of the initial MB concentration on the adsorbent, the initial MB concentrations were varied from 10 to 100 mg/mL at a time interval range of 2 min and 30 min, dose = 0.4 g/L, pH = 8, V = 25 mL, and shaking speed = 150 rpm. Figure 5a demonstrates how the removal percentage of MB decreased as the dye concentration increased from 10 mg/L to 100 mg/L, falling from 99.6% to 78%. The excessive amount of MB that exceeded the number of available adsorption sites is what caused the decrease in the dye removal percentage [27].

Figure 5b also suggests that the adsorption capacity increases with the increase in initial dye concentration until equilibrium is established. Figure 5b depicts that the adsorption capacity of MB dye increased from 24.9 mg/g to 195 mg/g with an increase in the initial dye concentration from 10 to 100 mg/L. The enhanced adsorption efficiency with increasing initial concentration might be corresponded to the high utilization of available vacant site on the surface and adsorption rate of MB dye adsorptions. This is due to the fact that at the higher initial dye concentration provides a more driving force which accelerates the mass transfer of adsorbate to the adsorbent

[28]. Thus, the initial dye concentration plays a significant role in the adsorption capacity of any adsorbate-adsorbent system. An initial MB dye concentration of 50 mg/L is chosen as the optimum condition for further studies.

Temperature

The effects of temperature on the rates of MB dye removal and its capacity for adsorption on the adsorbent were studied in experimental conditions of dose = 0.4 g/L, $C_0 = 50$ mg/L, pH = 8, time interval = 2 min-20 min, V = 25 mL, shaking speed = 150 rpm, and at different temperatures of 298 K, 303 K, and 313 K. Figures 5c and d demonstrate that the efficiency of removal and adsorption capacity of MB dye increased substantially from 94.5%, 118 mg/g (at 298 K), to 99.2%, 124.5 mg/g (at 303 K). This observation is explained by the fact that dye molecules are more mobile at higher temperatures, which causes a rise in dye molecule collisions and binding to *E. schimperi's* adsorption sites [29, 30]. The marginal rise in removal percentage (from 99.2% at 303 K to 99.8% at 313 K) and adsorption capacity (from 124.5 mg/g at 303 K to 124.75 mg/g at 313 K) are further indications of the endothermic nature of MB adsorption. However, at much higher temperatures (above 313 K), dye adsorption begins to decrease due to an increase in the dye molecule's Brownian motion and the breakdown of the intermolecular hydrogen bond between the dye molecules and the *E. schimperi's*, which may lead to dye molecule desorption from the surface of the *E. schimperi's*. Similar findings are described in the literature for the use of activated corn husk carbon in the adsorption of methylene blue [30].

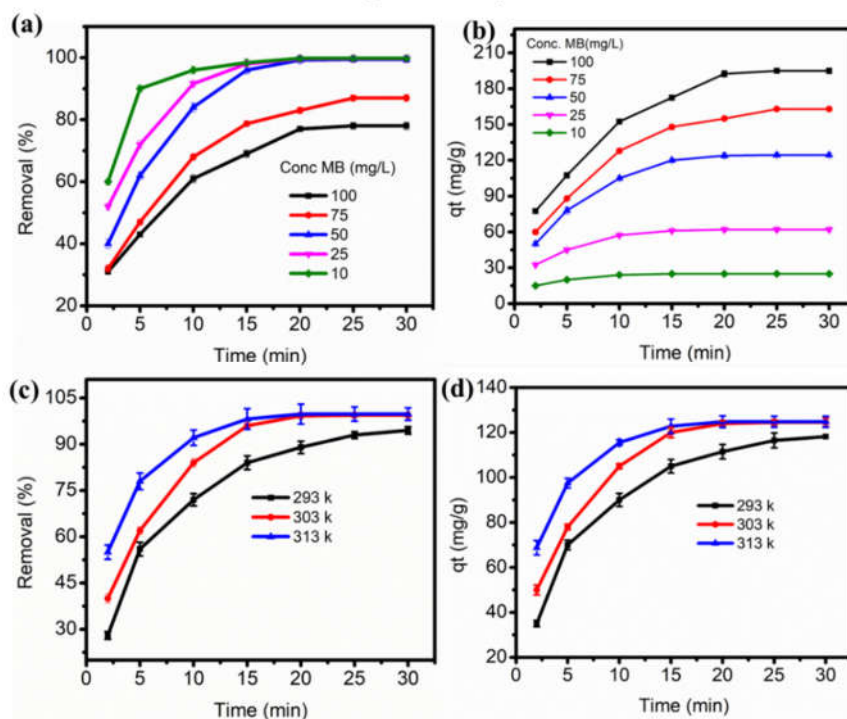


Figure 5. (a) The effect of initial concentration of MB dye on removal percentage; (b) The effect of initial concentration of MB dye on adsorption capacity; (c) The effect of temperature on removal percentage; and (d) The effect of temperature on adsorption capacity.

Adsorption isotherms analysis

Adsorption isotherms are useful models to describe the interaction between adsorbate and adsorbent in solution. The Langmuir and Freundlich adsorption isotherms [31, 32], two most prominent isotherm models describing the adsorbate-adsorbent interactions, were used to analyze the adsorption equilibrium over the entire concentration range from 10 mgL⁻¹ to 100 mgL⁻¹.

The linear form of Langmuir (Langmuir, 1918) and Freundlich isotherms are represented by Eqs. (4) and (5), respectively.

$$\frac{1}{q_e} = \frac{1}{q_m K_L C_e} + \frac{1}{q_m} \quad (4)$$

$$\ln q_e = \frac{1}{n} \ln C_e + \ln k_F \quad (5)$$

where C_e (mg/mL) is the equilibrium concentration, q_e (mg/g) is the equilibrium adsorption capacity, q_m (mg/g) is the maximum adsorption capacity of the Langmuir isotherm model, K_L (mL/mg) is a Langmuir adsorption coefficient, k_F (mL/mg) is the Freundlich constant, and $1/n$ is an indicator that reflects the nonlinear degree of adsorption.

The saturated monolayer is described by the Langmuir isotherm, while the saturated multilayer is characterized by the Freundlich isotherm [32]. As shown in Figures 6a and b, the slope and intercepts of linear plots of $1/q_e$ against $(1/C_e)$ and $\ln q_e$ against $\ln C_e$ for the Langmuir and Freundlich isotherm models, respectively, were used to evaluate all corresponding parameters, and the results are depicted in Table 1. Figures 6a and b show the Langmuir ($R^2 = 0.94899$) and Freundlich ($R^2 = 0.85738$) adsorption isotherm curves, and the linear analysis indicated that the observed dye adsorption data for *E. schimperii* was better described by the Langmuir isotherm model, as confirmed by the higher coefficient R^2 . This data suggests that monolayer adsorption occurs on a homogeneous surface with localized adsorption sites; similar observations were made for the MB adsorption onto the stem of canola and the adsorption onto PEI-wheat straw. Moreover, $1/n$ value (0.296) lies in the range of $0.1 < 1/n < 1$, the adsorption process is said to be favorable and feasible (Table 1). According to the Langmuir isotherm analysis, *E. schimperii* has a maximum adsorption capacity of 273.2 mg/g for MB dye. Based on this result, it seems that strong hydrogen bonds and electrostatic interactions play a key role in the chemical process known as chemisorption, which *E. schimperii* uses to adsorb the MB dye.

Adsorption kinetics studies

Pseudo-first-order and pseudo-second-order kinetics were used to evaluate the adsorption mechanism and predict the rate of dye removal from water. The linear form of first- and second-order kinetics is represented in Eqs. (6) and (7) respectively.

$$\ln(q_e - q_t) = \ln(q_e) - k_1 t \quad (6)$$

$$\frac{t}{q_t} = \frac{1}{K_2 q_e^2} + \frac{t}{q_e} \quad (7)$$

where q_e (mgg⁻¹) is the adsorption capacity at equilibrium, q_t (mgg⁻¹) is the adsorption capacity at time t (min), and k_1 (min⁻¹) and k_2 (gmg min⁻¹) are rate constants associated with pseudo first-order and pseudo second-order, respectively.

As shown in Figures 6c and d, the slope and intercepts of linear plots of $\ln(q_e - q_t)$ against (t) and t/q_t against (t) for pseudo-first-order and pseudo-second-order respectively, were used to evaluate all corresponding parameters, and the results are depicted in Table 2. The closeness of the linear correlation coefficient (R^2) to unity and agreement between q_{cal} and q_{exp} was used as a yardstick to dictate the best fitting kinetics for MB removal of dye from the test solution. As stated in Table 2, pseudo-first-order kinetics was unable to explain the adsorption of MB dye employed

in this study since the R^2 (0.94265) value is very low and there is a large difference between the values of q_{cal} (182.2 mg/g) and q_{exp} (124.5 mg/g). By contrast, pseudo-second-order kinetics is a suitable model describing the adsorption process considering a higher correlation coefficient ($R^2 = 0.99326$), and moreover, the q_{cal} (133.68 mg/g) values were more consistent with q_{exp} (124.5 mg/g), suggesting chemisorptions as the main factor in the rate of adsorption via strong ionic interaction between *E. schimperi* and MB dye molecules (Table 2). Literature indicates that the removal of MB by many biomass-based adsorbents like wheat straw [33], walnut shell powder [34], *Rumex abyssinicus* [34], *citrus limetta* peel [25], were well obeyed pseudo-second-order kinetic model.

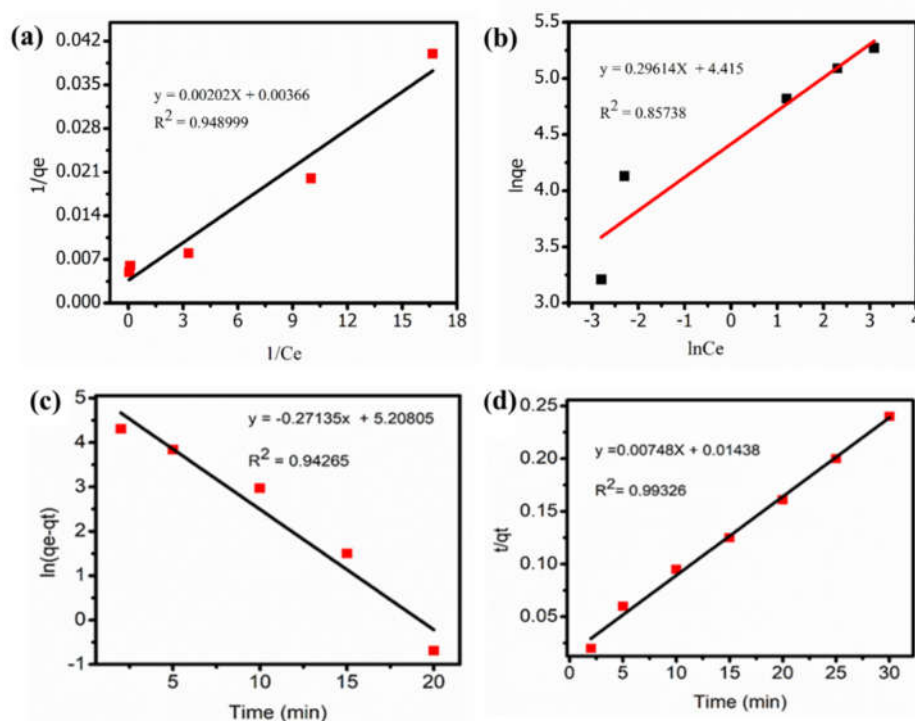


Figure 6. (a) Langmuir adsorption isotherm; (b) Freundlich adsorption isotherm; (c) Pseudo-first-order adsorption kinetics; and (d) Pseudo-second-order adsorption kinetics.

Table 1. The isothermal and kinetic parameters for the adsorption of MB onto *E. schimperi* biomass.

Isothermal models	Parameters	Values
Langmuir	q_m (mg/g)	273.2
	K_a (L/mg)	1.8
	R^2	0.94899
Freundlich	n	3.38
	$1/n$	0.296
	K_F (mg/g)	82.68
	R^2	0.85738

Table 2. The kinetics parameters for adsorption of MB onto *E. schimperi* biomass.

Kinetics models	Parameters	Values
Pseudo first order	k1 (min ⁻¹)	0.2713
	qe, calc (mg/g)	182.72
	qe, exp (mg/g)	124.5
	R ²	0.94265
Pseudo second order kinetic	k2 (g mg ⁻¹ min ⁻¹)	0.0039
	qe, calc (mg/g)	133.68
	qe, exp (mg/g)	124.5
	R ²	0.99326

Comparison with other adsorbents

Different bio-adsorbents such as fava bean peels, barley bran, nance seeds, eucalyptus tree, lemmon, palm tree, *Cucumis sativus* peel waste, modified soya wastes, and modified soya wastes are applied for the removal of MB from water. The efficiency of MB removal and the adsorption capacity (qe) of different adsorbents are shown in Table 3. According to the comparative adsorptions shown in Table 3, *E. schimperi*'s adsorbent is significantly more efficient than the other bio-adsorbents compared to previously reported extracts.

Table 3. The comparison between removal efficiency (%) and adsorption capacity (qe (mg/g)) of various adsorbents.

Adsorbents	Conditions	Removal (%) / qe (mg/g)	Reference
Fava bean peels	Dose: 5 g/L, conc: 3.6–25 mg/L, pH: 5	70–80%	[35]
Barley Bran	Dose: 2.5 g/L, conc: 10, mg/L, pH: 4-9, temp: 25 ± 1 ° C)	46% to 97% and 63.2 mg/g	[36]
Nance seeds	Dose: 0.1 g, conc: 25–250 mg/L, pH: 7 -10	98%	[37]
Eucalyptus tree	Dose: 2 g/L, conc: 5 mg/L, pH:8, time: 120 min, temp: 25 ° C	93.4%, 53.5 mg/g	[38]
Palm tree	Dose: 2 g/L, conc: 5 mg/L, pH:8, time: 120 min, temp: 25 ° C	95.8%, 54 mg/g	[38]
Lemmon	Dose: 2 g/L, conc: 5 mg/L, pH:8, time: 120 min, temp: 25 ° C	92.8%, 52.4 mg/g	[38]
<i>Cucumis sativus</i> peel waste	Dose: 0.4 g /L to 4 g/ L, L, pH: 8, time: 60 min	49.0% to 81.4% 122.4 mg/g to 20.4 mg/ g	[39]
Modified Soya wastes	Dose: 2 mg /6 mL, conc: 50 ppm, pH: 7, time: 15min, temp: 298 K	97.1% and 90 mg/g	[40]
<i>E. schimperi</i>	Dose: 0.4 g/L, conc: 50 mg/L, pH: 8, time: 20 min, temp 303 K	99.22% and 124.5 mg/g	This study

Antibacterial activities for crude extracts of *E. schimperi* fruits

In this study, the extract of the fruits of *E. schimperi* was investigated to evaluate its antibacterial activity against water-poising bacteria, including two strains of Gram-positive bacteria (LM and SA) and two strains of Gram-negative bacteria (EC and ST), using the disc diffusion method [41]. For Gram-positive bacteria, the diameters of the inhibition zone at different concentrations (25 to 100 mg/mL) were 10.55, 16.42, and 17.91 and 19.9 mm for LM and 10.31, 15.73, 16.74, and 17.42 mm for SA, and the averages of the four concentrations of LM and SA were 16.42 and 15.73, respectively, Table 4. Meanwhile, for the Gram-negative bacteria, the diameters of the inhibition zone at different concentrations (25 to 100 mg/mL) were 10.18, 14.78, 16.12, and 17.32 mm for EC and 8.72, 12.53, 13.77, and 14.97 mm for ST, and the averages of the four

concentrations of EC and ST were 14.78 mm and 12.53 mm, respectively. As a result, the average diameters of the inhibition zones showed a similar tendency toward increasing antibacterial efficiencies with increasing concentrations of *E. schimperi* from 25 mg/mL to 100 mg/mL. Hence, the average of four concentrations of *E. schimperi* was close to 50 mg/mL for Gram-positive and Gram-negative bacteria; the 50 mg/mL concentration was the appropriate one for the inhibition zone on the four bacteria (Table 4). *E. schimperi* crude extract was found to be effective with a concentration of 50 mg/mL against SA, LM, EC, and ST, suppressing their growth with inhibition zones of 16.42, 15.73, 14.78, and 12.53 mm, respectively.

Table 4. Bacterial growth zone of inhibition (mm) for the crude extract of *E. schimperi* fruits.

Concentration (mg/mL)	Average values of zone of inhibition (mm) ± SD							
	SA		LM		EC		ST	
25	10.31	1.07	10.55	0.82	10.18	1.43	8.72	0.52
50	15.73	0.95	16.42	1.09	14.78	0.80	12.53	0.72
75	16.74	0.72	17.91	0.87	16.12	1.03	13.77	0.72
100	17.42	1.19	19.93	1.27	17.32	1.27	14.97	0.65
Gen (10 µg/disc)	24.23	0.12	25.01	0.52	22.52	0.32	23.21	0.55
DMSO	-	-	-	-	-	-	-	-

LM = *Listeria monocytogenes*; SA = *Staphylococcus aureus*; ST = *Salmonella typhi*; EC = *Escherichia coli*; Gen = Gentamycin; DMSO = dimethylsulfoxide.

As indicated in Table 4, the crude extract of *E. schimperi* exhibited higher antibacterial activity against Gram-positive than Gram-negative bacteria but was less effective compared to that of gentamicin (22.52 to 25.01 mm zone of inhibition). DMSO did not show any activity against all the tested bacteria (Table 4). The results of the antimicrobial activity of the plant extracts suggest that ST was the most resistant strain to plant extracts, followed by EC, while SA and LM were the most susceptible strains to the extract plant, respectively. This might relate to differences in cell wall morphology between the two groups of bacteria. Gram-negative bacteria have an outer phospholipid membrane composed of lipo-polysaccharide constituents that make their cell wall impermeable to antimicrobial chemicals, whereas Gram-positive groups possess cell walls composed of a peptidoglycogen layer that is an inefficient permeability barrier.

The possible mechanisms for the fruit extract of *E. schimperi* to inhibit the four photogenes are explained by the fact that crude extracts contain secondary metabolites such as phenolic compounds, alkaloids, and flavonoids that penetrate cells to damage membranes, DNA, and the main functions of bacteria. Embelin (2, 5-dihydroxy-3-undecyl-p-benzoquinone) is an extract of *E. schimperi* known for its potent antibacterial properties against *S. aureus*, *S. pyogenes*, and *P. aeruginosa*. Hence, the broadest spectrum action on the four bacteria in the present study and the strong antimicrobial activity shown by extracts of *E. schimperi* fruit against SA and LM could be attributed to the existence of such active chemicals with pharmacological properties, further supporting the results of the phytochemical screening. The bioactivity of the extracts of the plants in this study is an indication of the potency of *E. schimperi* extract, which is not only used for the treatment of dyes but also to kill pathogens that are the cause of several waterborne diseases.

CONCLUSION

Major health and environmental issues are caused by the presence of toxic dyes and pathogens in water. The present investigation highlighted the simultaneous removal of MB dye and pathogenic bacteria from waste water using chloroform fruit extract of *E. schimperi* biomass, which is an inexpensive and environmentally friendly biosorbent and medicinal plant. AFM and FTIR

characterizations of the adsorbent showed that there was a change in morphology and shift in spectra of the functional groups of the adsorbents before and after the adsorption, respectively. Adsorption experiments were carried out in batches with varying adsorbent doses, contact time, pH values, initial MB concentrations, and temperatures. The optimum predicted conditions, which include a biomass concentration of 0.4 g/L, a contact time of 20 min, an initial pH level of 8, an initial MB dye concentration of 50 mg/L, and a temperature of 303 K, resulted in a nearly complete removal of MB dye (99.2%) from the aqueous solution. Besides this, Gram-positive and Gram-negative bacteria with different inhibition zones responded effectively to crude extracts of the fruits of *E. schimperi*. With a mean diameter of different inhibition zones, LM (16.42 mm) exhibited the highest antibacterial activity of *E. schimperi*, followed by SA (15.33 mm), EC (14.78 mm), and ST (12.53 mm). Therefore, the use of crude extracts of *E. schimperi* fruits for the biosorption of MB dye and antibacterial activity has been identified as a potential and practical alternative to remediation of pollutants as well as killing bacteria from wastewater simultaneously.

ACKNOWLEDGMENTS

The authors express their gratitude to Debre Berhan University for financial and material support.

REFERENCES

1. Bastaraud, A.; Cecchi, P.; Handschumacher, P.; Altmann, M.; Jambou, R. Urbanization and waterborne pathogen emergence in low-income countries: Where and how to conduct surveys? *Int. J. Environ. Res. Public Health* **2020**, *17*, 480.
2. Velusamy, S.; Roy, A.; Sundaram, S.; Kumar Mallick, T. A Review on heavy metal ions and containing dyes removal through graphene oxide-based adsorption strategies for textile wastewater treatment. *Chem. Res.* **2021**, *21*, 1570-1610.
3. Idrees, K.; Khalid, S.; Ivar, Z.; Baoliang, Z.; Abdulmajeed, H. H.; Ashfaq, A.; Shujaat, A.; Noor, Z.; Hanif, A.; Luqman, A. S.; Tariq, S.; Ibrahim, K. Review on methylene blue: Its properties, uses, toxicity and photodegradation. *Water* **2022**, *14*, 242.
4. Oladoye, P.O.; Ajiboye, T.O.; Omotola, E.O.; Oyewola, O.J. Methylene blue dye: Toxicity and potential elimination technology from wastewater. *Results Eng.* **2022**, *16*, 100678.
5. Tesfaw, B.; Chekol, F.; Mehretie, S.; Admassie, S. Adsorption of Pb(II) ions from aqueous solution using lignin from *Hagenia abyssinica*. *Bull. Chem. Soc. Ethiop.* **2016**, *30*, 473-484.
6. Chakma, S.; Das, L.; Moholkar, V.S. Dye decolorization with hybrid advanced oxidation processes comprising sonolysis/Fenton-like/photo-ferrioxalate systems: A mechanistic investigation. *Sep. Purif. Technol.* **2015**, *156*, 596-607.
7. Riera-Torres, M.; Gutiérrez-Bouzán, C.; Crespi, M. Combination of coagulation–flocculation and nanofiltration techniques for dye removal and water reuse in textile effluents. *Desalination* **2010**, *252*, 53-59.
8. Thanushree, M.S.; Mahadevaswamy, M.; Mahesh, S.; Sahana, M.; Chiranth, P. Electrochemical treatment of real cotton fabric industry wastewater using copper and stainless steel electrodes. *J. Water Sanit. Hyg. Dev.* **2023**, *13*, 197-207.
9. Gebreeyessus, G.D. Status of hybrid membrane–ion-exchange systems for desalination: A comprehensive review. *Appl. Water Sci.* **2019**, *9*, 135.
10. Agarwala, R.; Mulky, L. Adsorption of dyes from wastewater: A comprehensive review. *ChemBioEng Rev.* **2023**, *10*, 326-335.
11. Mo, J.; Yang, Q.; Zhang, N.; Zhang, W.; Zheng, Y.; Zhang, Z. A review on agro-industrial waste (AIW) derived adsorbents for water and wastewater treatment. *J. Environ. Manage.* **2018**, *227*, 395-405.

12. Ahmad, F. Ullah Shah, A. Biosorption of Ni(II) ions from aqueous solutions using *Melia azedarach* biomass. *Bull. Chem. Soc. Ethiop.* **2022**, 36, 521-530.
13. Abdul, M.; Abbas K.; Natasha, A.; Muhammad, N. A comparative study of the adsorption of Congo red dye on rice husk, rice husk char and chemically modified rice husk char from aqueous media. *Bull. Chem. Soc. Ethiop.* **2020**, 34, 41-54.
14. Ashbolt, N.J. Microbial contamination of drinking water and human health from community water systems. *Curr. Environ. Health Rep.* **2015**, 2, 95-106.
15. Cabral, J.P. Water microbiology. Bacterial pathogens and water. *Int. J. Environ. Res. Public Health.* **2010**, 7, 3657-3703.
16. Rondevaldova, J.; Leuner, O.; Tekla, A.; Lulekal, E.; Havlik, J.; Van Damme, P.; Kokoska, L. In vitro anti-staphylococcal effects of *Embelia schimperi* extracts and their component embelin with oxacillin and tetracycline. *Evid. Based Complement Alternat Med.* **2015**, 2015, 175983.
17. Lellis, B.; Fávoro-Polonio, C.Z.; Pamphile, J.A.; Polonio, J.C. Effects of textile dyes on health and the environment and bioremediation potential of living organisms. *Biotechnol. Res. Innov.* **2019**, 3, 275-290.
18. Yuan, L.; Yao, Q.; Liang, Y.; Dan, Y.; Wang, Y.; Wen, H.; Yang, Y.; Dan, W. Chitosan based antibacterial composite materials for leather industry: a review. *J. Leather. Sci. Eng.* **2021**, 3, 12.
19. Taiwo, A.S.; Adenike, K.; Aderonke, O. Efficacy of a natural coagulant protein from *Moringa oleifera* (Lam) seeds in treatment of Opa reservoir water, Ile-Ife, Nigeria. *Heliyon* **2020**, 6, e03335.
20. Guyasa, B.; Melaku, Y.; Endale, M. Antibacterial activity of two flavans from the stem bark of *Embelia schimperi*. *Adv. Pharmacol. Sci.* **2018**, 2018, 5870161.
21. Debebe, Y.; Tefera, M.; Mekonnen, W.; Abebe, D.; Woldekidan, S.; Abebe, A.; Belete, Y.; Menberu, T.; Belayneh, B.; Tesfaye, B.; Nasir, I.; Yirsaw, K.; Basha, H.; Dawit, A.; Debella, A. Evaluation of anthelmintic potential of the Ethiopian medicinal plant *Embelia schimperi* Vatke in vivo and in vitro against some intestinal parasites. *BMC. Complement. Altern. Med.* **2015**, 15, 187.
22. Kiprono, C.P.; Midiwo, J.O.; Kipkemboi, P.K.; Ladogana, S. Larvicidal benzoquinone from *Embelia Schimperi*. *Bull. Chem. Soc. Ethiop.* **2004**, 18, 45-49.
23. Wong, S.; Lee, Y.; Ngadi, N.; Inuwa, I.M.; Mohamed, N.B. Synthesis of activated carbon from spent tea leaves for aspirin removal. *Chin. J. Chem. Eng.* **2018**, 26, 1003-1011.
24. Garg, V. Basic dye (methylene blue) removal from simulated wastewater by adsorption using Indian rosewood sawdust: A timber industry waste. *Dyes Pigm.* **2004**, 63, 243-250.
25. Shakoor, S.; Nasar, A. Removal of methylene blue dye from artificially contaminated water using citrus limetta peel waste as a very low cost adsorbent. *J. Taiwan Inst. Chem. Eng.* **2016**, 66, 154-163.
26. Pavan, F.A.; Mazzocato, A.C.; Gushikem, Y. Removal of methylene blue dye from aqueous solutions by adsorption using yellow passion fruit peel as adsorbent. *Bioresour. Technol.* **2008**, 99, 3162-3165.
27. Mahmoudi, E.; Azizkhani, S.; Mohammad, A.W.; Ng, L.Y.; Benamor, A.; Ang, W.L.; Ba-Abbad, M. Simultaneous removal of Congo red and cadmium(II) from aqueous solutions using graphene oxide-silica composite as a multifunctional adsorbent. *J. Environ. Sci.* **2020**, 98, 151-160.
28. Jawad, A.H.; Hum N.N.M.F.; Farhan, A.M.; Mastuli, M.S. Biosorption of methylene blue dye by rice (*Oryza sativa* L.) straw: Adsorption and mechanism study. *Desalin. Water Treat.* **2020**, 190, 322-330.
29. Chakraborty, S.; Chowdhury, S.; Das Saha, P. Adsorption of crystal violet from aqueous solution onto NaOH-modified rice husk. *Carbohydr. Polym.* **2011**, 86, 1533-1541.

30. Badawi, A.K.; Abd Elkodous, M.; Ali, G. Recent advances in dye and metal ion removal using efficient adsorbents and novel nano-based materials: An overview. *RSC adv.* **2021**, *11*, 36528-36553.
31. Pan, Y.; Shi, X.; Cai, P.; Guo, T.; Tong, Z.; Xiao, H. Dye removal from single and binary systems using gel-like bioadsorbent based on functional-modified cellulose. *Cellulose* **2018**, *25*, 2559-2575.
32. Al-Ghouti, M.A.; Da'ana, D.A. Guidelines for the use and interpretation of adsorption isotherm models: A review. *J. Hazard. Mater.* **2020**, *393*, 122383.
33. Zhang, W.; Yan, H.; Li, H.; Jiang, Z.; Dong, L.; Kan, X.; Yang, H.; Li, A.; Cheng, R. Removal of dyes from aqueous solutions by straw based adsorbents: Batch and column studies. *J. Chem. Eng.* **2011**, *168*, 1120-1127.
34. Uddin, M.K.; Nasar, A. Walnut shell powder as a low-cost adsorbent for methylene blue dye: Isotherm, kinetics, thermodynamic, desorption and response surface methodology examinations. *Sci. Rep.* **2020**, *10*, 7983.
35. Bayomie, O.S.; Kandeel, H.; Shoeib, T.; Yang, H.; Youssef, N.; El-Sayed, M.M.H. Novel approach for effective removal of methylene blue dye from water using fava bean peel waste. *Sci. Rep.* **2020**, *10*, 7824.
36. Mekuria, D.; Diro, A.; Melak, F.; Asere, T.G.; Rehman, R. Adsorptive removal of methylene blue dye using biowaste materials: barley bran and enset midrib leaf. *J. Chem.* **2022**, *2022*, 4849758.
37. Robles-Melchor, L.; Cornejo-Mazón, M.; Hernández-Martínez, D.M.; Gutiérrez-López, G.F.; García-Pinilla, S.; López-Villegas, E.O.; Téllez-Medina, D.I.; Senturk, M. Removal of methylene blue from aqueous solutions by using nance (*Byrsonima crassifolia*) seeds and peels as natural biosorbents. *J. Chem.* **2021**, *2021*, 5556940.
38. Esmacili, H.; Foroutan, R. Adsorptive behavior of methylene blue onto sawdust of sour lemon, date palm, and eucalyptus as agricultural wastes. *J. Dispers. Sci. Technol.* **2018**, *40*, 990-999.
39. Shakoor, S.; Nasar, A. Adsorptive treatment of hazardous methylene blue dye from artificially contaminated water using cucumis sativus peel waste as a low-cost adsorbent. *Groundw. Sustain. Dev.* **2017**, *5*, 152-159.
40. Batool, A.; Valiyaveetil, S. Chemical transformation of soya waste into stable adsorbent for enhanced removal of methylene blue and neutral red from water. *J. Environ. Chem. Eng.* **2021**, *9*, 104902.
41. Bubonja-Sonje, M.; Giacometti, J.; Abram, M. Antioxidant and antilisterial activity of olive oil, cocoa and rosemary extract polyphenols. *Food Chem.* **2011**, *127*, 1821-1827.